

Free-space quantum key distribution with entangled photons

Ivan Marcikic, Antía Lamas-Linares, and Christian Kurtsiefer
Department of Physics, National University of Singapore, Singapore, 117542
(Dated: November 26, 2024)

We report on a complete experimental implementation of a quantum key distribution protocol through a free space link using polarization-entangled photon pairs from a compact parametric down-conversion source. Over 10 hours of uninterrupted communication between sites 1.5 km apart, we observe average key generation rates of 630 per second after error correction and privacy amplification. Our scheme requires no specific hardware channel for synchronization apart from a classical wireless link, and no explicit random number generator.

Quantum key distribution [1] is probably the most mature application developed out of quantum information science during the last decade. Based on initial ideas of Wiesner [2], quantum states of physical systems with small Hilbert spaces can be used to encode information in a way that an illegitimate attempt of accessing that information will result in a perturbation of the state, and consequently in revealing the interception attempt. Thus, the secrecy of a bit string or a key between two parties could be ensured relying on fundamental laws of quantum mechanics rather than assumptions on the mathematical complexity of problems like factoring.

A specific protocol to establish a secret key between two parties was established by Bennett and Brassard (BB84) [3], which used the polarization degree of freedom of single photons. An alternative scheme for a quantum optics based key distribution was suggested by Ekert [4], where nonlocal correlations in the measurements on entangled photon pairs both allow to establish a secret key and evaluate the knowledge of an eavesdropper out of a violation of Bell inequalities. In this scenario, only the detection units needed to be in possession of legitimate communication partners, while the entangled photon source need not to be in a trusted hand. Work on security analysis of quantum key distribution systems also typically makes use of entanglement, even in the case of the original or modified BB84 implementations with faint coherent pulses [5].

Practical implementations of quantum key distribution (QKD) can be classified according to the type of protocol and the physical transmission channel. We distinguish protocols of the prepare and send (PaS) type and entanglement based schemes. The transmission channel is either optical fiber or free space.

Most demonstrations of QKD (including all commercial systems) are PaS protocols implemented over fiber channels [6] and a few over free space [7]. The choice of channel reflects the maturity of fiber technology and its commercial possibilities in current networks. The preference for PaS protocols is due to the technological simplicity compared with entanglement based schemes. However, security in PaS protocols relies on the availability of high bandwidth trusted random numbers, which does not need to be the case for entanglement based systems.

First steps towards entanglement based QKD were experiments on distributing entanglement in the field over

fiber links [8] and in free space [9, 10]. More recently, QKD over a purposely laid fiber link was reported [11]. In this paper we describe a entanglement based (modified BB84) full field implementation of QKD over an ad hoc free space link. The system is based on a compact ($80 \times 50 \text{ cm}^2$) spontaneous parametric down-conversion source (SPDC), compact detection modules, a free space standard wireless internet protocol link and a software synchronization protocol taking advantage of intrinsic time correlations in the SPDC process. Error correction and privacy amplification are implemented on the fly producing a continuous stream of secure key.

A schematic experimental set-up is shown in figure 1. Light at 404nm emitted by a cw laser diode (LD) is circularized and focused (PO) to a waist of $90 \mu\text{m}$ into a β -barium borate (BBO) non-linear crystal. There, polarization-entangled photon pairs are created via type-II SPDC out of 50mW power. An additional half-wave plate (WP) and BBO crystals (CC) compensate walk-off effects [12, 13]. These crystals are also used to set the relative phase between horizontal (H) and vertical (V) polarizations such that the source produces photon pairs in a singlet Bell state:

$$|\Psi^-\rangle = \frac{1}{\sqrt{2}}(|H\rangle_A |V\rangle_B - |V\rangle_A |H\rangle_B)$$

Indices A and B (denoted Alice and Bob) represent two spatial modes defined by coupling SPDC light into single mode optical fibers (SMF) [13]. Center wavelength and spectral bandwidth are 805.2nm and 6.3nm for Alice's mode, and 810.7nm and 6.8nm for Bob's mode. Each fiber passes through a polarization controller (FPC) to undo fiber induced polarization transformations. At the source we observe a coincidence rate of $24\,000 \text{ s}^{-1}$ with an overall coupling and detection efficiency of 22 %, detected by passively quenched Silicon avalanche photo diodes (Si-APD). The entanglement quality is verified by measuring polarization correlations in H/V and $+45/-45$ basis. We observe a visibility of $98 \pm 2.6 \%$ and $92 \pm 2.2 \%$, respectively.

In a BB84-type QKD experiment, Alice's and Bob's polarization detection units (PA) randomly analyze the received photons in two maximally conjugated basis (H/V and $+45/-45$). For this purpose we use compact detection units [14] relying on a non-polarizing beam splitter (BS) to ensure the random choice of the measurement

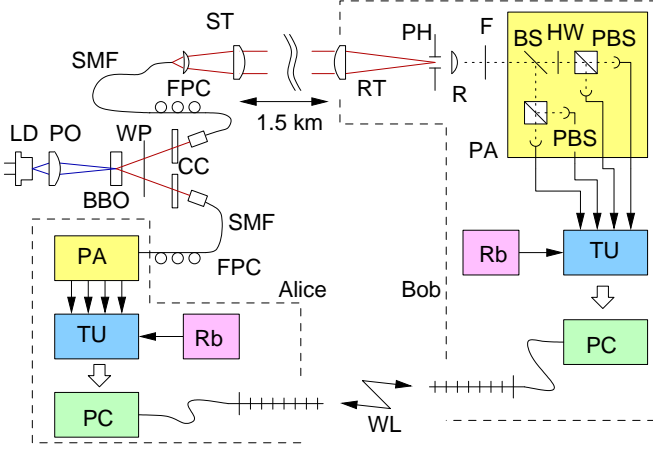


FIG. 1: Scheme of the experimental set-up. Polarization-entangled photons are distributed between two parties, Alice and Bob, separated by 1.5 km. Coincidence identification uses time-stamp units and requires a wireless link.

basis. Projection onto $+45/-45$ basis in the transmitted arm is via a half wave plate (HW) and polarizing beam splitter (PBS); in the reflected arm the H/V projection is implemented directly with a PBS. Photons are finally detected with four Si-APDs cooled to around -15°C (with outside $T=28^\circ\text{C}$) with an average dark count rate of 1000 s^{-1} per detector.

Optical ports are situated on the rooftops of two buildings in the campus of National University of Singapore (E103° 46' 48.3"; N1° 17' 48.7" and E103° 46' 3.5"; N1° 18' 8"), separated by 1.5 km. The entangled pair source is connected by 50 m of single-mode fiber to the sending telescope (ST) collimating the fiber mode into a Gaussian beam with a waist of 15 mm. The receiving telescope (RT, focal length of 310 mm, diameter 77 mm) focuses light onto a pinhole (PH) with $50\text{ }\mu\text{m}$ diameter acting as a spatial filter. An interference filter (F, $\lambda_0 = 810.7\text{ nm}$, FWHM= 5 nm) is used for background suppression. The pinhole is imaged (R) onto the Si-APDs in the polarization analyzer. The pointing accuracy of the telescopes is $\approx 10\text{ }\mu\text{rad}$.

In a protocol based on pairs of photons, it is fundamental to identify reliably which events are correlated in their times of arrival. With a cw laser pumped source, pair arrival times are random on all time scales, both due to the preparation process and the randomizing influence of losses. In lab experiments and some field implementations, coincidence or timing information required a dedicated hardware channel [10, 11]. In our experiment, we use a software-based coincidence identification, where we continuously register the detection time of all photo-events on both sides with a timestamp unit (TU) locked to a Rb oscillator [9, 14, 15].

Before coincidences can be identified, the clocks on both sides need to be synchronized to the order of a coincidence time window. We start with a standard NTP protocol [16] between the controlling hosts (PC in fig. 1)

to an accuracy $< 100\text{ ms}$, followed by a tiered cross correlation on raw photodetection timings. Initial locking of the remote clocks takes a few seconds to extract coarse and fine timing information with a resolution of $2.048\text{ }\mu\text{s}$ and 2 ns , respectively, followed by an FFT algorithm to find the maxima of the cross correlation functions.

For efficient timing communication, we partition detection events in packets every 2^{29} ns and encode time intervals between consecutive events, reaching a bandwidth $\approx 13\%$ above the Shannon limit or 1 Mbit per second for 50 000 events per second. Timing information consumes the largest bandwidth of all communication on the classical channel, but is comparable to schemes with a fixed timing raster which would not allow to work efficiently with a cw pumped source. We used a standard 801.11g wireless connection (WL) for classical communication.

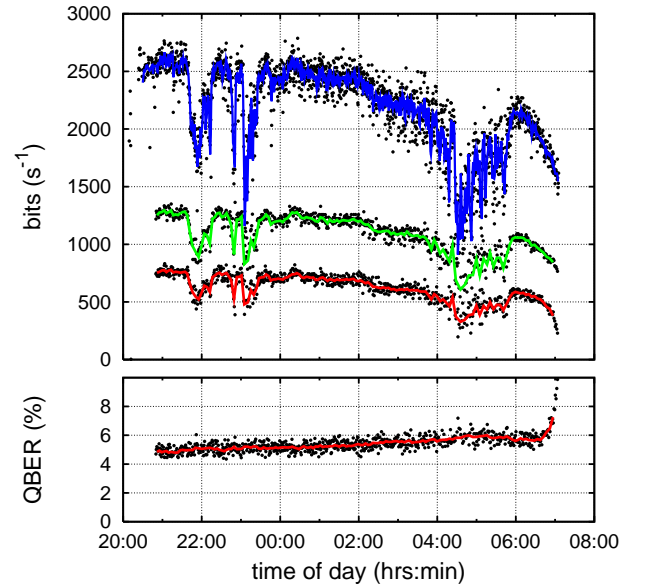


FIG. 2: Quantum key distribution between two sites 1.5 km apart. In the top panel, the traces correspond to the raw coincidence rates between the remote sites, sifted and final secure key after error correction and privacy amplification. The bottom panel shows the measured quantum bit error ratio of the sifted key. The acquisition took place during an uninterrupted period of ≈ 10 hours at night. The reduced scatter in the sifted and error corrected keys is due to the clustering of the data for error correction and privacy amplification. For clarity, the traces show a downsampled (1 out of 10) subset.

The coincidence identification is carried out asynchronously on the high count rate side. Due to timing jitter of photodetectors, reference clock noise, clock drift servo noise, and noise in time stamp units, we observe a cumulative width of 1.4 ns (FWHM) for the distribution of coincidence time differences Δt . For raw key generation, we accept coincidences with $|\Delta t| < 1.75\text{ ns}$. Coincidences with $|\Delta t| < 3.75\text{ ns}$ are used to servo the clock drifts for continuous operation beyond the reference clock stability, which would only allow for only a few minutes of operation. Accidental coincidences (8.63 s^{-1} in

average between 21:00 and 06:00 hours) monitored in a 3.75 ns wide reference window displaced by 20 ns from the main coincidence window are consistent with total single event rates on transmitter side ($99\,692\text{ s}^{-1}$) and receiver side ($18\,325\text{ s}^{-1}$) detectors. To ensure that different timing delays of individual detectors could not be exploited for eavesdropping, we equalized the average delays to $\approx 0.25\text{ ns}$.

We remove errors in the raw key on the fly with a modified CASCADE/BICONF error correction algorithm (following largely [17]) on clusters of collated raw key packets with at least 5 000 bits. The required bandwidth on the classical communication channel is small compared to the initial sifting.

Privacy amplification [18] for obtaining s secure key bits out of r raw key bits in a cluster removes possible knowledge of an eavesdropper out of an attack (estimated from the observed error fraction η in the raw key), and due to the c revealed parity bits in the error correction process. We assume an attack-based knowledge of an eavesdropper of $e = r/2[(1+z)\log_2(1+z) + (1-z)/\log_2(1-z)]$, with $z = 2\sqrt{\eta(1-\eta)}$. The compression matrix for privacy amplification to $m = r - e - c$ final key bits is generated on the fly from a publicized seed for a pseudo random number generator for every cluster. All observed errors are assigned to an eavesdropping attempt, no assumptions on the inability of an eavesdropper to access intrinsic errors in the system are made.

Our results are presented in figure 2. The initial remote coincidence rate is $2\,600\text{ s}^{-1}$ and drops to $2\,000\text{ s}^{-1}$ after $\approx 10\text{ hrs}$ without any intervention or active stabilization after initial alignment. The secret key exchange is finally interrupted by the rising sun saturating the detectors. The quantum bit error ratio (QBER), i.e. the ratio between wrong over correct events, increases slowly from $\approx 5\%$ to $\approx 6\%$, with an overall average of 5.4% . We do not observe any appreciable increase in QBER due to the propagation through the atmosphere. We attribute the small increase of 0.5% between the local and remote QBER to residual uncompensated birefringence in the fiber connecting the source to the telescope. Af-

ter the basis reconciliation the averaged sifted and secret keys bit rates are $1\,100\text{ s}^{-1}$ and 630 s^{-1} . Our error correction implementation resulted in a residual bit error ratio (BER) of 2×10^{-5} in this run, clearly bunching in particular clusters. After privacy amplification, this lead to 230 clusters with nonidentical final key out of 7 500.

The remote coincidence rate is around 11 % of the local rate. We observe a transmission between the entangled pair source and the sending telescope of 85 %, through telescope optics 90 % and through interference filter 50 %. Separation of 1.5 km leads to an additional signal reduction of 50 %. Each detection unit exhibits another 20 % of losses. We do not observe a significant contribution to the losses due to scintillation.

For a second experiment, we replace the interference filter with a long pass filter (RG780). Over 6 hours of measurement, around 850 bits per second of secret key are distributed on average. The sifted key bit rate increases to $1\,600\text{ s}^{-1}$ with an average QBER of 5.75% . The BER before privacy amplification was 2×10^{-6} on cluster sizes $> 10\,000$ bits, leading to 21 nonidentical key out of 1 720 after privacy amplification.

In conclusion, we have demonstrated a real-time free-space quantum key distribution based on a BB84-type protocol with polarization-entangled photons. A software base coincidence identification scheme was implemented, not relying on a dedicated hardware channel. A nighttime experiment with an interference filter ran uninterruptedly for over 10 hours producing an average secure key rate of 630 bits per second, while with a long pass filter we observed 850 bits per second over 6 hours. We believe that this QKD set-up can be used even for daylight operation: from preliminary experiments we estimate that the accidental coincidence rate therefore must be reduced by one order of magnitude, which can be achieved with stronger spectral and spatial filtering, and a shorter coincidence time window.

The authors acknowledge the DSTA Singapore for their financial support and thank Darwin Gosal, Gleb Maslennikov, Alexander Ling, Hou Shun Poh and Meng Khoon Tey for their help.

-
- [1] N. Gisin, G. Ribordy, W. Tittel and H. Zbinden, *Rev. Mod. Phys.* **74**, 145 (2002)
 - [2] S. Wiesner, *Sigact News* **15**, 78 (1983)
 - [3] C. Bennett and G. Brassard, in *Proceedings of the IEEE Int. Conf. On Computer Systems and Signal Processing (ICSSSP)*, publisher Bangalore, India (1984), 175
 - [4] A. Ekert, *Phys. Rev. Lett.* **67**, 661 (1991)
 - [5] P. W. Shor and J. Preskill, *Phys. Rev. Lett.* **85**, 441 (2000); N. Lutkenhaus, *Phys. Rev. A* **61**, 052304 (2000)
 - [6] R. J. Hughes, G. L. Morgan, and C. G. Peterson, *J. Mod. Opt.* **47**, 533 (2000); D. Stucki, N. Gisin, O. Guinnard, G. Ribordy and H. Zbinden, *New J. Phys.* **4**, 41 (2002); C. Gobby, Z. L. Yuan, and A. J. Shields, *Appl. Phys. Lett.* **84**, 3762 (2004)
 - [7] R. J. Hughes, W. T. Buttler, P. G. Kwiat, S. K. Lamoreaux, G. L. Morgan, J. E. Nordholt, and C. G. Peterson, *J. Mod. Opt.* **47**, 549 (2000); J. G. Rarity, P. M. Gorman, and P. R. Tapster, *Electron. Lett.* **37**, 512 (2001)
 - [8] W. Tittel, J. Brendel, H. Zbinden, and N. Gisin, *Phys. Rev. Lett.* **81**, 3563 (1998)
 - [9] K. J. Resch, M. Lindenthal, B. Blauensteiner, H. R. Böhm, A. Fedrizzi, C. Kurtsiefer, A. Poppe, T. Schmitt-Manderbach, M. Taraba, R. Ursin, P. Walther, H. Weier, H. Weinfurter, and A. Zeilinger, *Opt. Express* **13**, 202 (2005)
 - [10] C.-Z. Peng, T. Yang, X.-H. Bao, J. Zhang, X.-M. Jin, F.-Y. Feng, B. Yang, J. Ying, Q. Zhang, N. Li, B.-L. Tian, and J.-W. Pan, *Phys. Rev. Lett.* **95**, 030502 (2005)

- [11] A. Poppe, A. Fedrizzi, T. Lorünser, O. Maurhardt, R. Ursin, H. R. Böhm, M. Peev, M. Suda, C. Kurtsiefer, H. Weinfurter, T. Jennewein, and A. Zeilinger, *Opt. Express* **12**, 3865 (2004)
- [12] P. G. Kwiat, K. Mattle, H. Weinfurter, A. Zeilinger, A. V. Sergienko, and Y. Shih, *Phys. Rev. Lett.* **75**, 4337 (1995)
- [13] P. Trojek, C. Schmid, M. Bourennane, H. Weinfurter, and C. Kurtsiefer, *Opt. Express* **12**, 276 (2004)
- [14] C. Kurtsiefer, P. Zarda, M. Halder, H. Weinfurter, P. M. Gorman, P. R. Tapster, and J. G. Rarity, *Nature* **419**, 450 (2002)
- [15] T. Jennewein, C. Simon, G. Weihs, H. Weinfurter, and A. Zeilinger, *Phys. Rev. Lett.* **84**, 4729 (2000)
- [16] D. L. Mills, *IEEE Trans. Communications COM-39* **10**, 1482 (1991)
- [17] G. Brassard and L. Salvail, in *Advances in Cryptology - Proc. Eurocrypt'94*, pp. 410-423 (1994); T. Sugimoto and K. Yamazaki, *IEICE Trans. Fundamentals* **E83-A**, 1987 (2000)
- [18] C. H. Bennett, G. Brassard and J.-M. Robert, *SIAM J. Comput.* **17**, 210 (1988)